A Cohesin-RAD21 Interactome

Anil K. Panigrahi, Nenggang Zhang, Subhendu K. Otta, Debananda Pati[1]

Texas Children's Cancer Center, Department of Pediatric Hematology/Oncology, Baylor College of Medicine, 1102 Bates Avenue, Suite 1220 Houston, TX, 77030, USA

The cohesin complex holds the sister chromatids together from S phase until the metaphase-to-anaphase transition and ensures both their proper cohesion and timely separation. In addition to its canonical function in chromosomal segregation, cohesion has been suggested by several lines of investigation in recent years to play additional roles in apoptosis, DNA damage response, transcriptional regulation, and hematopoiesis. To better understand the basis of the disparate cellular functions of cohesin in these various processes, we have characterized a comprehensive protein interactome of cohesin-RAD21 by using three independent approaches: yeast 2-hybrid (Y2H) screening, immunoprecipitation-coupled-mass spectrometry (IP-M) of cytoplasmic and nuclear extracts from MOLT-4 T lymphocytes in the presence and absence of etoposide induced apoptosis, and affinity-pull down assays of chromatographically purified chromatin extracts from proapoptotic MOLT-4 cells. Our analyses revealed 112 novel protein interactors of cohesin RAD21 that function in different cellular processes including mitosis, regulation of apoptosis, chromosome dynamics, replication, transcription regulation, RNA processing, DNA damage response, protein modification and degradation, and cytoskeleton and cell motility. Identification of cohesin interactors provides a framework for explaining the various non-canonical functions of the cohesin complex.

Short Title: A Cohesin-RAD21 Interactome

Key words: Cohesin, RAD21, sister chromatid cohesion, apoptosis

[1]To whom correspondence should be addressed (email pati@bcm.tmc.edu)

Footnote: Abbreviations used: CE, cytoplasmic extract; DDR, DNA damage response; IP, immunoprecipitation; IP-M, immunoprecipitation-coupled mass spectrometry; LC-MS/MS, liquid chromatography-coupled tandem mass spectrometry; NE, nuclear extract; WCL, whole cell lysate; Y2H, yeast two-hybrid

INTRODUCTION

The sister chromatids generated in the S-phase must stay cohered in order to facilitate chromosomal bi-orientation prior to segregation into the daughter cells. Such cohesion between the sister chromatids is mediated by the tripartite cohesin ring, formed by two *s*tructural *m*aintenance of *c*hromosome proteins SMC1A and SMC3, and the α-kleisin subfamily protein RAD21 [1-3]. Another non-SMC *s*tromal *a*ntigen protein (one of SA1, SA2, and SA3), homolog of the budding yeast Scc3p, also is associated invariably with, and is considered an integral component of, the cohesin ring [4, 5]. At different stages of the cell cycle, several other proteins also dynamically associate with cohesin and regulate both cohesion and separation of sister chromatids; these include sororin/CDCA5, PDS5A and PDS5B, WAPAL, SGOL1, and Separase [6-8]. In early prophase of the vertebrate cell cycle, cohesin is removed from the chromosomal arms in a reaction dependent on the kinase PLK1 and the cohesin interactor WAPAL [9-11]. Once the chromosomes are properly bi-orientated, the residual cohesin from the centromeres is removed in a reaction dependent on proteolytic cleavage of RAD21 by the endopeptidase Separase [9, 12]. Altered expression of both Separase and RAD21 [13-16] as well as inactivating mutations in cohesin component SA2 [17] can lead to genomic instability and have been implicated in tumorigenesis ([13, 14, 16, 18, 19]; see [20] for a recent review).

Apart from coordination of sister chromatid cohesion and separation, the cohesin complex has also been shown to contribute to various other chromosomal functions [6, 21] including gene regulation [22-24]. Horsfield et al [25] reported a mutant strain of zebrafish, Nz171, which lacks all hematopoietic RUNX1 expression in early embryogenesis and demonstrates defective hematopoiesis. They determined that the gene underlying Nz171 was *rad21*. These findings provide evidence that cohesin plays a role in hematopoiesis and development. Subtle mutations in cohesin components that apparently don't affect the chromosomal cohesion can cause an altered transcriptome and have been associated with human diseases [22]. Furthermore, cohesin also plays important roles in the DNA damage response (DDR) pathway [26, 27]. Whereas post-replicative recruitment of cohesin is important for the repair of DNA double-strand breaks [28], RAD21 haploinsufficiency confers a DNA damage defect and sensitivity to ionizing radiation [29]. Investigations in the past few years have also shed significant light on the role of cohesin in DNA replication [30]. Cohesin directly interacts with proteins involved in DNA replication [31], organizes the architecture of replicating chromatin [32], and accelerates replication processivity [33]. In addition to the various critical roles it plays in chromosome biology, cohesin is involved in apoptosis. The cohesin component RAD21 is cleaved during apoptosis [29, 34], and the C-terminal fragment of RAD21 is thought to translocate to the cytoplasm to accelerate the apoptotic response [34].

How cohesin coordinates such diverse functions in the cell is not clear. A simple notion would posit that cohesin physically interacts with various proteins within disparate cellular microenvironments to regulate diverse cellular functions, and identification of a cohesin interactome would shed light on the mechanisms of cohesin function. To test the above hypothesis, we have attempted to characterize comprehensively the cohesin-protein interactome in human cells. We took three independent approaches: a yeast 2-hybrid screen with RAD21 as the bait, an immunoprecipitation-coupled-mass spectrometry analysis for RAD21-bound proteins, and a RAD21-affinity pull-down assay to identify RAD21-interacting proteins. Our results reveal a number of novel protein interactors of RAD21 with a known or projected role in pathways as diverse as chromosome dynamics, mitosis, apoptosis, DNA repair, splicing, protein translation and degradation, cytoskeleton function and metabolism. Several of these interactors have a known role in carcinogenesis.

MATERIALS AND METHODS

Yeast 2-hybrid screen: The screen was conducted as described elsewhere [35]. Full length (FL, 1-631aa), N-terminal (NT, 1-282aa), C-terminal long (CTl, 254-631aa) and C-terminal short (CTs, 283-631aa) versions of *RAD21* ORF were sub-cloned in frame with Gal4 DNA-binding domain (Gal4DBD) in a pPC97 vector (bait). An activated human T cell cDNA library in a Gal4 activation domain (Gal4AD) fusion vector pPC86 was used as prey in the screening along with the baits. More than $3x10^6$ colonies were screened for each transformation.

Cell culture and transfection: MOLT-4 cells were grown in RPMI-1640 with 10% fetal bovine serum (FBS). HeLa and HEK293T cells were grown in DMEM plus 10% FBS. Flag- (pFlag CMV2), HA- (pCruz-HA) and Myc- (pCS2MT) tagging vectors were used to generate the expression constructs for the selected proteins and transfected into HEK293T cells using calcium phosphate method as described [11]. When applicable, MOLT-4 cells were treated with 25 μM etoposide for 4 hr (for RAD21 cleavage assay and affinity pull-down experiments, see below) or with 10 μM for 12 hr (for immunoprecipitation-coupled mass spectrometric identification of RAD21-interactors).

Cell fractionation and immunoprecipitation-coupled mass spectrometry: Cytoplasmic extracts (CE) were prepared by hypotonic lysis of cells with hypotonic buffer (HB) (10 mM Tris-HCl, pH 7.8, 10mM NaCl, 1.5 mM $MgCl_2$ supplemented with 0.2% Igepal) into cytoplasmic and nuclear fractions. Nuclear pellets were extracted (nuclear extract, NE) with NETN buffer (25mM Tris-HCl, pH 7.8, 150 mM NaCl, 1mM EDTA, 0.5% Igepal). Total soluble proteins were prepared by extracting cells with NETN. The residual pellet was resuspended in NETN and fragmented by sonication to prepare the chromatin fraction. Cellular fractions were immunoprecipitated with anti-RAD21 antibody as described [36]. The immunoprecipitated proteins were resolved by SDS-PAGE, and gel slices were processed for tryptic digestion and liquid chromatography-coupled tandem mass spectrometric (LC-MS/MS) analysis by the Proteomics Core Facility at Baylor College of Medicine, Houston, TX.

Antibodies and Western blotting: Western blotting was performed as described [37]. Rabbit polyclonal and mouse monoclonal antibodies against RAD21 have been described before [34]. The following other antibodies were used at indicated dilutions: anti-HA (H6908; 1:10000), anti-DAPK3/Zip kinase (Z0134; 1:1000) were from Sigma-Aldrich, Saint Louis, MO; anti-CDC34 (C25820; 1:1000) was from Transduction Laboratories, Lexington, KY; anti-PPM1D (A300-664A; 1:1000), anti-SMC2 (A300-058A; 1:2000), anti-NCAPG (A300-602A; 1:2000), anti-DDB1 (A300-462A-1; 1:1000), p30/DBC1 (A300-434A; 1:4000), anti-EWS1 (A300-417K; 1:5000) were from Bethyl Laboratories, Montgomery, TX; anti-tubulin (CP06-100UG; 1:5000) from Oncogene Research Products, Cambridge, MA; anti-Lamin B (ab16048; Abcam, Cambridge, MA; 1:2000); anti-SMC1A (sc-10707; 1:1000), anti-GADD34 (sc-8327; 1:000) were from Santa Cruz Biotechnology, Santa Cruz, CA; anti-UBA1 (NB600-472; 1:1000) was from Novus Biologicals, Littleton, CO.

Assay and partial purification of RAD21 cleavage activity: Myc.RAD21 substrate was synthesized from pCS2MT-RAD21 plasmid in a wheat-germ extract-based transcription-coupled-translation (TnT, Promega, Madison, WI) reaction. NE from apoptotic MOLT-4 cells were prepared as described above, but in a different buffer (PP buffer-300: 25mM Tris-HCl, pH 8.0, 5% glycerol, 1.5mM $MgCl_2$, 0.2% Igepal, supplemented with 300 mM NaCl). For RAD21 cleavage assay, NE and fractions from chromatographic steps (see below) were incubated with Myc.RAD21 for 2hr at 37°C and were analyzed by Western blotting using an anti-RAD21 antibody that recognizes the C-terminus. The active fractions generated a 64kD band reminiscent

of *in vivo* apoptotic fragmentation as previously described [34]. For partial purification of the RAD21 cleavage activity, NE was diluted 1:3 PP buffer-0 (with no salt) and passed through a Uno Q1 column (1 ml, Bio-Rad, Hercules, CA). The flow-through was bound to and eluted from a Uno S1 column (1 ml, Bio-Rad) in a 0.1-0.5M NaCl gradient in PP buffer. Active fractions showing RAD21 cleavage activity were pooled, concentrated and fractionated on a Superdex 200 column in PP buffer-150. The chromatographic operations were performed using a BioLogic DuoFlow system FPLC (Bio-Rad, Hercules, CA).

Affinity pull-down: RAD21 matrix was generated by immobilizing Myc.RAD21 (from TnT reaction) onto anti-Myc agarose beads. The active fraction #30 from the Superdex 200 column was pre-cleared with anti-Myc agarose beads and then bound to anti-myc agarose beads (mock) or RAD21 matrix. The beads were washed with PP buffer-150 and resolved by SDS-PAGE. The entire gel was stained with Coomassie blue and cut into slices. LC-MS/MS was performed on the all gel slices by Nextgen Sciences, Ann Arbor, MI.

Bioinformatic analysis: Identified proteins were analyzed using publicly available DAVID (the database for annotation, visualization and integrated discovery) for functional classification [38]; functional annotation clustering of the list of RAD21 interactors was performed with medium classification stringency. Protein-protein interaction network was visualized using STRING (search tool for the retrieval of interacting genes/proteins) [39]. STRING presents each protein node as a circle, the size of which is automatically generated; the larger size only reflects that there is structural information associated with the protein. When available, the structure of the protein is embedded as a thumbnail within the circle. Multiple protein IDs (Uniprot Accession numbers) were analyzed with medium confidence setting (0.400). Gene/protein identity mapping was performed manually or at Uniprot (www.uniprot.org). The lists of interactors were examined by MEROPS database to identify a protease (http://merops.sanger.ac.uk/).

RESULTS

Yeast 2-hybrid screening

We have reported previously that RAD21 is cleaved at D279 by an unknown caspase-like protease during apoptosis, and the C-terminal fragment (283-631aa) translocates to the cytoplasm to further aid in the apoptotic response [34]. Therefore, we were interested in finding protein interactors that specifically bind the N-terminal or the C-terminal fragments of RAD21. RAD21 also has a region (257-360aa) with strong homology to TNFR, a member of the Tumor Necrosis Factor (TNF)-receptor superfamily with a known role in mediating apoptosis. Since the mechanism of RAD21-mediated instigation of the apoptotic response is unknown, we hoped that inclusion of this 257-360aa region might also identify some specific interactors. Therefore, we used two versions of C-terminal RAD21 as baits.

The screen using FL RAD21 identified 18 positive clones, while the screen with NT RAD21 identified 3 positive clones (Table 1), and all of these clones were in frame with the Gal4AD. We obtained several positive clones with the CTl and CTs RAD21 screens, but none was in frame with the Gal4AD. The validity of the screening result is reflected by the identification of SMC1A as a RAD21 interactor. SMC1A joins with RAD21 and SMC3 to form the tripartite ring of the mitotic cohesin complex. Our screen also identified several RAD21 fragments as RAD21 interactors indicating self association of RAD21 molecules, which has been previously described [36] and further confirming the validity of this Y2H screen. Of the total 21 ORFs identified, all but SMC1A are novel interactors of RAD21. Functional annotation analysis performed using DAVID revealed five proteins that are involved in apoptosis: DAPK3,

PPP1R15A/GADD34, TNFRSF14, CSTB and CFL1. The other proteins identified are involved in diverse processes including protein synthesis, protein degradation, splicing, transcription and signaling. We reconfirmed the interactions in candidate-specific Y2H experiments (data not shown). As an alternate validation, we generated epitope-tagged versions of some of the identified ORFs, co-expressed them in HEK293T cells along with RAD21, and performed immunoprecipitation (IP) experiments. As shown in Figure 1, RAD21 physically interacts with FHL3 (Figure 1A), CDC34 (Figure 1B) and DAPK3 (Figure 1D).

Additionally, we took a candidate-based approach to find novel RAD21 interactors. One such candidate is the phosphatase Wip1/PPM1D, which functions in the DNA damage response pathway (DDR). PPM1D has also been suggested to dephosphorylate SMC1A [40]. Therefore, we wanted to verify its interaction with RAD21. As shown in Figure 1C, PPM1D and RAD21 interact when overexpressed.

IP-mass spectrometric analysis

Our Y2H assay identified a few RAD21-interacting proteins that could only be validated using overexpressed proteins. Considering the inherent drawbacks of the Y2H assays including overexpression of the constructs and potential for false positives/negatives, we embarked on a biochemical approach to identify physiological interactors of RAD21 using endogenous RAD21 IP followed by mass spectrometry analyses. We performed several IP experiments using an antibody raised against the C-terminus of RAD21 [34] (see schematic in Figure 2A). First, RAD21 was immunoprecipitated from the CE prepared from normal as well as apoptotic acute lymphoblastic leukemia cells MOLT-4. As previously shown [34], RAD21 is normally a nuclear protein, but is cleaved during apoptosis and its C-terminal fragments translocate to cytoplasm (see Figure 2B, compare lane 1 to 2). Immunoprecipitation from the untreated CE was thus considered both as a negative control for the IP and as a tool to access sticky proteins that might cross-react with the anti-RAD21 antibody. The immunoprecipitates were subjected to mass spectrometric analyses to identify the proteins. All four canonical components of the cohesin complex (RAD21, SMC1A, SMC3, SA2) were identified in the immunoprecipitate from the apoptotic CE, while no cohesin components were detected in the immunoprecipitate from the etoposide-untreated CE (Suppl. Table S1). Several proteins were also detected only in the immunoprecipitate from the cohesin-deficient untreated CE, indicating that they somehow cross-react with anti-RAD21 antibody (Suppl. Table S1). These proteins were therefore considered non-specific and were excluded from further analysis. We also prepared CE and NE from HeLa cells and performed immunoprecipitation using anti-RAD21 antibody. RAD21 is usually not present in the cytosol (Figure 2B), and thus the immunoprecipitation from HeLa CE served as an additional negative control. We identified in the NE immunoprecipitate all components of the canonical cohesin complex, known cohesin-associated proteins including PDS5A and WAPAL, as well as novel cohesin-interactors including nucleosome assembly protein 1-like 1 (Nap1L1), replication factor C (RFC3) and condensin component NCAPG (see Suppl. Table S2). However, no cohesin component was detected in the immunoprecipitate from the CE.

Because RAD21 and the cohesin complex exist in the cell both as a soluble pool and as a chromatin-bound fraction, and the only other proteolytic processing of RAD21 known to occur is during apoptosis, our aim was to identify RAD21 interactors from total soluble proteins and from the insoluble chromatin-enriched fraction from cells treated with or without etoposide. Table 2 lists the proteins identified from the immunoprecipitates from both the soluble and chromatin fractions. Proteins with two or more peptides retrieved from the mass spectrometry were taken into consideration. This analysis detected all the components of the canonical cohesin complex as well as the known cohesin interactors PDS5A, PDS5B and WAPAL that regulate both

chromatin-cohesin interaction and resultant sister chromatid cohesion. Additionally, this analysis also revealed several novel interactors that supposedly function in a microenvironment related to cohesin. For example, cohesin has been shown to be important for DDR [34, 35], and our analysis identified damaged DNA binding protein DDB1 as a RAD21 interactor. The replication licensing and execution machinery, along with the clamp proliferating cell nuclear antigen (PCNA) and various replication factor C complexes (RFCs, loader and unloader of the PCNA clamp); have been proposed to function in conjunction with cohesin and cohesion establishment. We identified several replication licensing factors (MCM2, MCM3, MCM4 and MCM7 isoform 1 and 2) as well as PCNA as RAD21 interactors, while identification of RFC3 has been mentioned above. Interestingly, our analysis also identified the chromodomain ATPase CHD4/Mi2β as a novel interactor of RAD21. CHD4 is highly similar to CHD3/Mi2α, which is a known interactor of RAD21 [41]. Apart from these, several other proteins were also identified as novel RAD21 interactors that supposedly function in a wide variety of cellular pathways (see Table 2).

We used the STRING database [39] to analyze all the RAD21-interactors excluding contaminating proteins (Figure 2C). STRING plots the listed proteins (nodes) based on the strength of internodal interactions, which is comprised of protein-protein binding (black lines) as well as functional interactions other than binding (grey lines). Here, we included five highly predicted proteins in the analysis that are selected automatically by the program based on the input list of proteins. The five proteins automatically added to this list include Flap endonuclease FEN1, Cyclin-dependent kinase inhibitor CDKN1A, replication factor C component RFC1 and DDB1-interacting partners CUL4A and DDB2 (all underlined; Figure 2C). Our analysis predicts cohesin components SMC1A and SMC3 to interact with FEN1, RFC1 and PCNA, whereas PCNA would further link with the replication licensing factors (Fig 2C). Importantly, we later identified both FEN1 and CUL4A as specific RAD21 interactors in a different experiment with an independent approach (see below). Another interesting observation is the physical interaction of transcription regulator THO complex component 4 (THOC4) with RAD21. THOC4 has been found to interact with SMC1A [42]. THOC4 also interacts with TPR and the importin KPNB1, the nuclear pore and nuclear transport components that we also found to physically interact with RAD21. Three distinct hubs are apparent in the STRING analysis: Cohesin and cohesin-related proteins, UBC, DDB1 and UBA1-related ubiquitin-proteasome pathway proteins, and the MCM-RFC-related pro-replication proteins. This finding is significant because cohesin has been implicated in both replication and DDR.

As depicted in Fig 3, several of the interactors were experimentally validated for their interaction with RAD21 using endogenous protein IP. They include DDB1, p30/DBC1/KIAA1967, PPP1R15A/GADD34 and Ewing sarcoma protein EWS1 (Figure 3A). We observed both DDB1 (which is part of the CUL4A ubiquitin ligase complex) and the ubiquitin-activating enzyme UBA1 (E1) bind to RAD21 and to each other (Figure 3B). We also observed UBA1, EWS1 and DDB1 immunoprecipitating each other (data not shown), the biological significance of which is currently under investigation. Figure 3C further demonstrates that RAD21 and p30/DBC1 can co-immunoprecipitate each other.

Affinity pull-down

RAD21 is proteolytically cleaved during mitosis by the endopeptidase Separase [12], but the identity of the protease responsible for the apoptotic cleavage of RAD21 is unclear [34]. In our IP-mass spectrometry investigations into RAD21 interactors, as described above, we did not identify any protease that interacted with RAD21. Therefore, we used an affinity pull-down approach geared towards identifying a RAD21 protease and additional RAD21-binding proteins during apoptosis. We generated a RAD21 affinity matrix by immobilizing *in vitro* translated Myc.RAD21 onto anti-Myc agarose beads. RAD21-cleaving activities in the apoptotic NE from MOLT-4 cells was enriched over three chromatographic steps and finally was bound to the

RAD21 matrix as well as to anti-myc agarose beads (see schematic in Figure 4A, and RAD21 cleavage assay in Figure 4B). The bound proteins were subjected to LC/MS-MS analysis. Supplemental Table S3 lists all 97 proteins that specifically bound to the Myc.RAD21 matrix but not to the Myc beads (Mock), for which a minimum of two peptides were retrieved. This list has an enormous abundance of ribosomal proteins and translation factors. In order not to overwhelm our analysis by the abundant sticky ribosomal proteins which have been identified in many other IP-mass spectrometry analyses, we excluded these proteins, plus HSP90A chaperone, from further consideration. These proteins are listed in Supplemental Table S3.

Since the goal of this experiment was to identify a RAD21-proteinase, we first focused on the ubiquitous protease Calpain-1 (CAPN1; two peptides were retrieved in the analysis). We verified that Calpain-1 cleaves RAD21 *in vitro* and *ex vivo* upon calcium treatment, but not during apoptosis. The site of Calpain-1 cleavage (L192) is different from the apoptotic cleavage (D279), and this cleavage promotes sister chromatid separation [37]. The characterization of Calpain-1 as a bona fide RAD21 interactor validates our affinity purification approach. The only other probable protease (according to the MEROPS database) identified in this experiment is the CAD protein, which actually is a fusion of four biochemical activities: GATase (glutamine amidotransferase), CPSase (carbamoyl phosphaste synthase), ATCase (aspartate carbamoyl transferase) and DHOase (dihydroorotase).

We also identified four components of the human condensin I complex, namely SMC2, SMC4, NCAPG and NCAPD2. NCAPG was also identified in one of the RAD21-IP experiments (Suppl. Table S2). Currently, a notion of physical interaction between condensin and cohesin has not been appreciated. Therefore, we decided to verify if such physical interactions between RAD21 and condensins do exist. We immunoprecipitated RAD21 from normal or apoptotic MOLT-4 whole cell lysates (WCL) and observed two endogenous condensin I components, SMC2 and NCAPG, co-immunoprecipitating with RAD21 (Figure 4C). Interestingly, we also observed proteolytic truncation of NCAPG (marked with an asterisk; Figure 4C) in the apoptotic WCL.

Also consistent with the bioinformatic prediction as depicted in Fig 2C, we identified the flap endonuclease FEN1 as a specific interactor of RAD21. STRING predicts interaction of FEN1 with topoisomerase III alpha (TOP3A) and DDB1, both of which, along with the DDB1-partner CUL4A, were identified as specific direct interactors of RAD21 in this analysis.

Analysis of this list of proteins by DAVID revealed only 5 proteins involved in apoptosis: RAD21 itself, Calpain-1, API5, CUL4A and tubulin beta 2C (TUBB2C).

DISCUSSION

Cohesin has been implicated in a vast range of cellular processes apart from sister chromatid cohesion and separation. It is possible that cohesin communicates with several proteins that function in different cellular processes. For instance, cohesin interacts with the spindle pole associated factor NuMA and colocalizes with the spindle poles [43]. The entire cohesin complex also has been reported to interact with the nuclear matrix [43, 44]. Recently, cohesin has been reported to interact with Aire, a master regulator of the expression of peripheral tissue self-antigens [45]. Several other proteins, such as the splicing factor SKIP/SNW1 [46], the schizophrenia risk gene product DISC1 [47] and the *Yersinia pestis* pathogen protein Y2928 [48] also have been suggested to interact with cohesin. However, no elaborate investigation into protein interactors of cohesin has been performed. Here we report characterization of the cohesin protein interactome, which we identified by using principal cohesin subunit RAD21 as the bait.

Using three different approaches, Y2H, IP-M and Affinity-pull-down, we identified 112 novel interactors of RAD21, several of which were validated in immunoprecipitation experiments. As Table 3 depicts, these proteins largely fall into 10 classes, with some overlaps, based on the cellular processes in which they are involved. We identify previously unsuspected processes such as protein modification and degradation, cytoskeleton and cell motility, RNA processing and nucleocytoplasmic trafficking in which RAD21-interacting proteins play a role. These results suggest the involvement of RAD21 in vastly different cellular processes beyond sister chromatid cohesion and separation. Our analysis reveals several important nodal hubs of known physical interactions within the RAD21 interactome. The foremost is the cohesin complex along with its known associated proteins, condensin-I and chromatin modifiers (Figure 5A). The other important hubs identified include replication associated proteins (Figure 5B), protein ubiquitination and deubiquitination (Figure 5C), transcription and RNA metabolism (Figure 5D), and cytoskeleton and cell motility (Figure 5E). Interestingly, the entire cohesin complex has recently been shown to interact physically with the MCM complex [32]. We analyzed the entire 112 interactors using STRING database along with 12 known RAD21 interactors (not identified from our screen): Caspase 7, NUMA1, SMARCA5/SNF2H, AIRE, CDCA5/sororin, CHD3/Mi2β, CHTF18/CHL12, CTCF, SRRM1/SRM160, ESPL1/Separase, DISC1 and SKIP/SNW1. Several proteins within this composite network are known to interact with each other (Suppl. Figure S1). The replication hub appears to connect a further set of nodal hubs, including ubiquitin-proteasome pathway proteins UBC-UBA1-CUL4A-DDB1 and splicing regulators YBX1-DHX9-SYNCRIP-HNRNPH1 (Supplemental Figure S1). DHX9 further communicates with transcription regulator THOC4, Ewing sarcoma protein EWS1, cohesin (SMC1A) and also with the nuclear matrix protein SRRM1 (not identified in our screen). SRRM1 forms a major hub communicating with the transcription regulator THOC4, nuclear transport proteins TPR and KPNB1, mitotic spindle stabilizer NUMA. The chromodomain chromatin remodeler CHD4 is also a transcription regulator, and appears to communicate with SRRM1, THOC4, RFCs and p30/DBC1 (Supplemental Figure S1). YBX1 is also a transcription factor important for hematopoiesis [49]. Identification of the putative transcription factor ZNF80 as a RAD21-interactor may lead to important clues to cohesin's role in transcription regulation. While trying to grasp the significance of all these inter-nodal and inter-hub interactions, it is important to note that each node shown here actually interacts with cohesin (RAD21) directly.

Another point of interest depicted by the RAD21 interactome as presented here (Figure 5C) is the physical interaction of RAD21 with several components of the ubiquitin system. CDC34, which is described above as a novel RAD21 interactor (Table 1; Figure 1B), is an E2 ubiquitin conjugating enzyme. RAD21 also pulls down another E2 enzyme, UBE2O (Figure 5C; Supplemental. Table S3). Identification of the Ubiquitin activating enzyme E1 (UBA1) and the E3 ligases DDB1-CUL4A and UBE3C further make a compelling case that RAD21 functions in

the ubiquitin pathway. This finding is consistent with a recent report that both SMC1A and SMC3 interact with several proteins of the deubiquitination pathway [42].

One of the objectives of this work was to understand the mechanism of RAD21-mediated apoptosis by identifying Rad21 interactors. RAD21 is cleaved during apoptosis, but the responsible protease for this cleavage remains unknown [34]. Although we were not able to identify a bona fide protease that cleaves Rad21 during apoptosis, we indentified a number of RAD21-interacting proteins with direct or indirect role in apoptosis (see Table 3). Apoptosis requires chromatin condensation and fragmentation, and apoptotic cleavage of cohesin RAD21 is thought to play a role therein. In the current work, we uncover human condensin I complex as physically interacting with cohesin RAD21. This is important for two reasons. First, a notion of physical communication between cohesins and condensins did not exist until recently, when the cohesin, condensin and the chromosomal passenger complex were reported to cooperate in spindle dynamics in yeast [50]. Second, even though cohesin is a known proteolytic target during mitosis and apoptosis, similar proteolytic processing of a condensin component is unknown. Our observation of proteolytically cleaved condensin I component NCAPG in apoptotic WCL raises critical questions as to why cohesin and condensin components are cleaved during apoptosis and whether such cleavage is mechanistically linked to apoptotic chromatin condensation and fragmentation. This also emphasizes the need to identify the protease that cleaves cohesin and condensin during apoptosis. A protease-substrate interaction is meant to be transient, and the approaches taken here were inadequate to capture the protease. Use of a bioactive protein-cross linker may help identifying the protease.

Identification of a set of novel interactors of cohesin presents enormous promise to the field of cohesin biology. The amount of information that can be generated by experimental validation of each of these interactors and elucidation of the biological significances is exemplified by Calpain-1. It can be noted that Calpain-1 (CAPN) was identified as a specific interactor of RAD21 and remains as an unconnected peripheral node (Supplemental Figure S1). However, this identification led to the discovery that Calpain-1 indeed cleaves RAD21 at a precise site (L192), causes loss of cohesin from chromatin, and consequently promotes separation of chromosomal arms [37]. Likewise, characterization of other interactors might reveal new facets of cohesin's function. However, it must be noted that the entire interactome characterization was performed using MOLT-4 cells, and the actual interactome may differ in different cell types. Moreover, it is possible that several of the interactions reported here may be dynamic in reference to cell cycle stages and may also change during the course of differentiation.

In summary, we have characterized a comprehensive protein interactome for the cohesin RAD21 and identified 112 proteins that interact with RAD21. These proteins function in diverse sets of pathways and processes. However, the majority of the uncovered interactions with RAD21/cohesin await experimental validation, which will shed new light on the mechanism of cohesin function in global cellular pathways.

AUTHOR CONTRIBUTIONS:

Conceived the idea and obtained the grant support: DP. Designed the experiments: DP AP NZ. Performed the experiments: DP AP SO NZ. Analyzed the data: AP DP NZ SO. Wrote the paper: AP DP.

ACKNOWLEDGEMENTS

We thank Subhashree Pradhan (Baylor College of Medicine, Houston, TX) for technical assistance. We thank Dr. Lisa Wang for critically reading the manuscript and Dr. Betty Ligon for editing the text. This study was supported by grants awarded to D. Pati from the National Cancer Institute (1RO1 CA109478).

REFERENCES

1 Michaelis, C., Ciosk, R. and Nasmyth, K. (1997) Cohesins: chromosomal proteins that prevent premature separation of sister chromatids. Cell. **91**, 35-45
2 Guacci, V., Koshland, D. and Strunnikov, A. (1997) A direct link between sister chromatid cohesion and chromosome condensation revealed through the analysis of MCD1 in S. cerevisiae. Cell. **91**, 47-57
3 Haering, C. H., Lowe, J., Hochwagen, A. and Nasmyth, K. (2002) Molecular architecture of SMC proteins and the yeast cohesin complex. Mol. Cell. **9**, 773-788
4 Losada, A., Yokochi, T., Kobayashi, R. and Hirano, T. (2000) Identification and characterization of SA/Scc3p subunits in the Xenopus and human cohesin complexes. J. Cell Biol. **150**, 405-416
5 Sumara, I., Vorlaufer, E., Gieffers, C., Peters, B. H. and Peters, J. M. (2000) Characterization of vertebrate cohesin complexes and their regulation in prophase. J. Cell Biol. **151**, 749-762
6 Peters, J. M., Tedeschi, A. and Schmitz, J. (2008) The cohesin complex and its roles in chromosome biology. Genes Dev. **22**, 3089-3114
7 Onn, I., Heidinger-Pauli, J. M., Guacci, V., Unal, E. and Koshland, D. E. (2008) Sister chromatid cohesion: a simple concept with a complex reality. Annu. Rev. Cell Dev Biol. **24**, 105-129
8 Nasmyth, K. and Haering, C. H. (2009) Cohesin: its roles and mechanisms. Annu. Rev. Genet. **43**, 525-558
9 Waizenegger, I. C., Hauf, S., Meinke, A. and Peters, J. M. (2000) Two distinct pathways remove mammalian cohesin from chromosome arms in prophase and from centromeres in anaphase. Cell. **103**, 399-410
10 Kueng, S., Hegemann, B., Peters, B. H., Lipp, J. J., Schleiffer, A., Mechtler, K. and Peters, J. M. (2006) Wapl controls the dynamic association of cohesin with chromatin. Cell. **127**, 955-967
11 Zhang, N., Panigrahi, A. K., Mao, Q. and Pati, D. (2011) Interaction of Sororin with Polo-like Kinase 1 Mediates the Resolution of Chromosomal Arm Cohesion. J. Biol. Chem. (In Press)
12 Hauf, S., Waizenegger, I. C. and Peters, J. M. (2001) Cohesin cleavage by separase required for anaphase and cytokinesis in human cells. Science. **293**, 1320-1323
13 Xu, H., Yan, M., Patra, J., Natrajan, R., Yan, Y., Swagemakers, S., Tomaszewski, J. M., Verschoor, S., Millar, E. K., van der Spek, P., Reis-Filho, J. S., Ramsay, R. G., O'Toole, S. A., McNeil, C. M., Sutherland, R. L., McKay, M. J. and Fox, S. B. Enhanced RAD21 cohesin expression confers poor prognosis and resistance to chemotherapy in high grade luminal, basal and HER2 breast cancers. Breast Cancer Res. **13**, R9

14 Meyer, R., Fofanov, V., Panigrahi, A., Merchant, F., Zhang, N. and Pati, D. (2009) Overexpression and mislocalization of the chromosomal segregation protein separase in multiple human cancers. Clin. Cancer Res. **15**, 2703-2710
15 Mukherjee, M., Ge, G., Zhang, N., Huang, E., Nakamura, L. V., Minor, M., Fofanov, V., Rao, P. H., Herron, A. and Pati, D. (2011) Separase Loss of Function Cooperates with the Loss of p53 in the Initiation and Progression of T- and B-Cell Lymphoma, Leukemia and Aneuploidy in Mice. PLoS One. **6**, e22167
16 Zhang, N., Ge, G., Meyer, R., Sethi, S., Basu, D., Pradhan, S., Zhao, Y. J., Li, X. N., Cai, W. W., El-Naggar, A. K., Baladandayuthapani, V., Kittrell, F. S., Rao, P. H., Medina, D. and Pati, D. (2008) Overexpression of Separase induces aneuploidy and mammary tumorigenesis. Proc. Natl. Acad. Sci. U S A. **105**, 13033-13038
17 Solomon, D. A., Kim, T., Diaz-Martinez, L. A., Fair, J., Elkahloun, A. G., Harris, B. T., Toretsky, J. A., Rosenberg, S. A., Shukla, N., Ladanyi, M., Samuels, Y., James, C. D., Yu, H., Kim, J. S. and Waldman, T. (2011) Mutational inactivation of STAG2 causes aneuploidy in human cancer. Science. **333**, 1039-1043
18 Porkka, K. P., Tammela, T. L., Vessella, R. L. and Visakorpi, T. (2004) RAD21 and KIAA0196 at 8q24 are amplified and overexpressed in prostate cancer. Genes Chromosomes Cancer. **39**, 1-10
19 Yamamoto, G., Irie, T., Aida, T., Nagoshi, Y., Tsuchiya, R. and Tachikawa, T. (2006) Correlation of invasion and metastasis of cancer cells, and expression of the RAD21 gene in oral squamous cell carcinoma. Virchows Arch. **448**, 435-441
20 Xu, H., Tomaszewski, J. M. and McKay, M. J. Can corruption of chromosome cohesion create a conduit to cancer? Nat. Rev. Cancer. **11**, 199-210
21 Merkenschlager, M. (2010) Cohesin: a global player in chromosome biology with local ties to gene regulation. Curr. Opin. Genet. Dev. **20**, 555-561
22 Liu, J., Zhang, Z., Bando, M., Itoh, T., Deardorff, M. A., Clark, D., Kaur, M., Tandy, S., Kondoh, T., Rappaport, E., Spinner, N. B., Vega, H., Jackson, L. G., Shirahige, K. and Krantz, I. D. (2009) Transcriptional dysregulation in NIPBL and cohesin mutant human cells. PLoS Biol. **7**, e1000119
23 Dorsett, D. (2010) Gene regulation: the cohesin ring connects developmental highways. Curr. Biol. **20**, R886-888
24 Kagey, M. H., Newman, J. J., Bilodeau, S., Zhan, Y., Orlando, D. A., van Berkum, N. L., Ebmeier, C. C., Goossens, J., Rahl, P. B., Levine, S. S., Taatjes, D. J., Dekker, J. and Young, R. A. (2010) Mediator and cohesin connect gene expression and chromatin architecture. Nature. **467**, 430-435
25 Horsfield, J. A., Anagnostou, S. H., Hu, J. K., Cho, K. H., Geisler, R., Lieschke, G., Crosier, K. E. and Crosier, P. S. (2007) Cohesin-dependent regulation of Runx genes. Development. **134**, 2639-2649
26 Watrin, E. and Peters, J. M. (2006) Cohesin and DNA damage repair. Exp. Cell Res. **312**, 2687-2693
27 Lehmann, A. R. (2005) The role of SMC proteins in the responses to DNA damage. DNA Repair (Amst). **4**, 309-314
28 Strom, L., Lindroos, H. B., Shirahige, K. and Sjogren, C. (2004) Postreplicative recruitment of cohesin to double-strand breaks is required for DNA repair. Mol. Cell. **16**, 1003-1015

29 Chen, F., Kamradt, M., Mulcahy, M., Byun, Y., Xu, H., McKay, M. J. and Cryns, V. L. (2002) Caspase proteolysis of the cohesin component RAD21 promotes apoptosis. J. Biol. Chem. **277**, 16775-16781
30 Sherwood, R., Takahashi, T. S. and Jallepalli, P. V. (2010) Sister acts: coordinating DNA replication and cohesion establishment. Genes Dev. **24**, 2723-2731
31 Ryu, M. J., Kim, B. J., Lee, J. W., Lee, M. W., Choi, H. K. and Kim, S. T. (2006) Direct interaction between cohesin complex and DNA replication machinery. Biochem. Biophys. Res. Commun. **341**, 770-775
32 Guillou, E., Ibarra, A., Coulon, V., Casado-Vela, J., Rico, D., Casal, I., Schwob, E., Losada, A. and Mendez, J. (2010) Cohesin organizes chromatin loops at DNA replication factories. Genes Dev. **24**, 2812-2822
33 Terret, M. E., Sherwood, R., Rahman, S., Qin, J. and Jallepalli, P. V. (2009) Cohesin acetylation speeds the replication fork. Nature. **462**, 231-234
34 Pati, D., Zhang, N. and Plon, S. E. (2002) Linking sister chromatid cohesion and apoptosis: role of Rad21. Mol. Cell. Biol. **22**, 8267-8277
35 Pati, D., Meistrich, M. L. and Plon, S. E. (1999) Human Cdc34 and Rad6B ubiquitin-conjugating enzymes target repressors of cyclic AMP-induced transcription for proteolysis. Mol. Cell. Biol. **19**, 5001-5013
36 Zhang, N., Kuznetsov, S. G., Sharan, S. K., Li, K., Rao, P. H. and Pati, D. (2008) A handcuff model for the cohesin complex. J. Cell Biol. **183**, 1019-1031
37 Panigrahi, A. K., Zhang, N., Mao, Q. and Pati, D. (2011) Calpain-1 cleaves rad21 to promote sister chromatid separation. Mol. Cell. Biol. **31**, 4335-4347
38 Huang da, W., Sherman, B. T. and Lempicki, R. A. (2009) Systematic and integrative analysis of large gene lists using DAVID bioinformatics resources. Nat. Protoc. **4**, 44-57
39 Szklarczyk, D., Franceschini, A., Kuhn, M., Simonovic, M., Roth, A., Minguez, P., Doerks, T., Stark, M., Muller, J., Bork, P., Jensen, L. J. and von Mering, C. (2011) The STRING database in 2011: functional interaction networks of proteins, globally integrated and scored. Nucleic Acids Res. **39**, D561-568
40 Yamaguchi, H., Durell, S. R., Chatterjee, D. K., Anderson, C. W. and Appella, E. (2007) The Wip1 phosphatase PPM1D dephosphorylates SQ/TQ motifs in checkpoint substrates phosphorylated by PI3K-like kinases. Biochemistry. **46**, 12594-12603
41 Hakimi, M. A., Bochar, D. A., Schmiesing, J. A., Dong, Y., Barak, O. G., Speicher, D. W., Yokomori, K. and Shiekhattar, R. (2002) A chromatin remodelling complex that loads cohesin onto human chromosomes. Nature. **418**, 994-998
42 Sowa, M. E., Bennett, E. J., Gygi, S. P. and Harper, J. W. (2009) Defining the human deubiquitinating enzyme interaction landscape. Cell. **138**, 389-403
43 Gregson, H. C., Schmiesing, J. A., Kim, J. S., Kobayashi, T., Zhou, S. and Yokomori, K. (2001) A potential role for human cohesin in mitotic spindle aster assembly. J. Biol. Chem. **276**, 47575-47582
44 McCracken, S., Longman, D., Marcon, E., Moens, P., Downey, M., Nickerson, J. A., Jessberger, R., Wilde, A., Caceres, J. F., Emili, A. and Blencowe, B. J. (2005) Proteomic analysis of SRm160-containing complexes reveals a conserved association with cohesin. J. Biol. Chem. **280**, 42227-42236
45 Abramson, J., Giraud, M., Benoist, C. and Mathis, D. Aire's partners in the molecular control of immunological tolerance. Cell. **140**, 123-135

46 Lleres, D., Denegri, M., Biggiogera, M., Ajuh, P. and Lamond, A. I. (2010) Direct interaction between hnRNP-M and CDC5L/PLRG1 proteins affects alternative splice site choice. EMBO Rep. **11**, 445-451

47 Camargo, L. M., Collura, V., Rain, J. C., Mizuguchi, K., Hermjakob, H., Kerrien, S., Bonnert, T. P., Whiting, P. J. and Brandon, N. J. (2007) Disrupted in Schizophrenia 1 Interactome: evidence for the close connectivity of risk genes and a potential synaptic basis for schizophrenia. Mol. Psychiatry. **12**, 74-86

48 Dyer, M. D., Neff, C., Dufford, M., Rivera, C. G., Shattuck, D., Bassaganya-Riera, J., Murali, T. M. and Sobral, B. W. (2010) The human-bacterial pathogen protein interaction networks of Bacillus anthracis, Francisella tularensis, and Yersinia pestis. PLoS One. **5**, e12089

49 Bhullar, J. and Sollars, V. E. (2011) YBX1 expression and function in early hematopoiesis and leukemic cells. Immunogenetics. **63**, 337-350

50 Li, Z., Vizeacoumar, F. J., Bahr, S., Li, J., Warringer, J., Vizeacoumar, F. S., Min, R., Vandersluis, B., Bellay, J., Devit, M., Fleming, J. A., Stephens, A., Haase, J., Lin, Z. Y., Baryshnikova, A., Lu, H., Yan, Z., Jin, K., Barker, S., Datti, A., Giaever, G., Nislow, C., Bulawa, C., Myers, C. L., Costanzo, M., Gingras, A. C., Zhang, Z., Blomberg, A., Bloom, K., Andrews, B. and Boone, C. (2011) Systematic exploration of essential yeast gene function with temperature-sensitive mutants. Nat. Biotechnol. **29**, 361-367

RAD21 Bait	Identified Proteins	Uniprot AC	Processes
FL	SMC1A	Q14683	Sister chromatid cohesion, DNA damage response, mitosis
FL	CDC34	P49427	Protein modification, Protein degradation
FL	RPL13	P26373	Protein synthesis
FL	RPL10	P27635	Protein synthesis
FL	WNT2B/Wnt13	Q93097	Developmental signaling
FL	HNRNPH2/FTP-3	P55795	Splicing/RNA processing
FL	PPP1R15B	Q5SWA1	Protein modification, Transcription regulation
FL	PPP1R15A/GADD34	O75807	Apoptosis; translation regulation
FL	DAPK3	O43293	Mitosis; regulation of apoptosis
FL	ZNF80	P51504	Putative transcription factor
FL	TNFRSF14	Q8N634	Apoptosis; immune response
FL	TMSB4X	P62328	Cytoskeleton/cell motility
FL	COX2	P00403	Metabolism
FL	IL7R	P16871	Immune response
FL	Cystatin-B	P04080	Proteinase inhibitor; regulation of apoptosis
FL	Filamin B	O75369	Cytoskeleton/cell motility
FL	Cofilin1	P23528	Cytoskeleton/cell motility
FL	MSRB2/CBS1	Q9Y3D2	Methionine metabolism
NT	FHL3	Q13643	Transcription; Cytoskeleton/cell motility
NT	DYNLT1/TCTEL1	P63172	Cytoskeleton/cell motility; intracellular transport
NT	RPL35A	P18077	Protein synthesis

TABLE 1. RAD21 Interactors identified from Yeast 2-hybrid (Y2H) Screening. 21 ORFs were identified from the Y2H screening using full length (FL) or N-terminal (NT) hRAD21. Uniprot Accession numbers (Uniprot AC) for the corresponding ORFs are listed.

Proteins	Description	Untreated*		Etoposide*		Uniprot AC	Processes
		Sol.	Chr.	Sol.	Chr.		
RAD21	Double-strand-break repair protein RAD21 homolog	583	478	321	161	O60216	Sister chromatid cohesion, DNA damage response, motosis
SMC1A	Structural maintenance of chromosomes protein 1A	527	475	759	606	Q14683	Sister chromatid cohesion, DNA damage response, motosis
SMC3	Structural maintenance of chromosomes protein 3	647	626	916	919	Q9UQE7	Sister chromatid cohesion, DNA damage response, motosis
SA1	Cohesin subunit SA-1	41	30	76	79	Q8WVM7	Sister chromatid cohesion, DNA damage response, motosis
SA2	Cohesin subunit SA-2	276	134	411	280	Q8N3U4	Sister chromatid cohesion, DNA damage response, motosis
PDS5B	Sister chromatid cohesion protein PDS5 homolog B	80	8	79	14	Q9NTI5	Sister chromatid cohesion, motosis
WAPAL	Wings apart like (Drosophila)	98	27	22	4	Q7Z5K2	Sister chromatid cohesion, motosis
PHACTR4	phosphatase and actin regulator 4 Isoform 2	15	4	7	4	Q8IZ21	Protein modification, Cytoskeleton/cell motility
UBC	ubiquitin C	2	1		4	P0CG48	Protein modification, Protein degradation
TPM3	tropomyosin 3	14	1			P06753	Cytoskeleton/cell motility
KPNB1	karyopherin (importin) beta 1	2	4			Q14974	Nucleocytoplasmic trafficking
C6orf97	hypothetical protein LOC80129; FLJ23305	12	2			Q8IYT3	Uncharacterized
UBA1	Ubiquitin-activating enzyme E1	6		10	1	P22314	Protein modification, Protein degradation
DDB1	damage-specific DNA binding protein 1, 127kDa	39		8		Q16531	DNA damage response, Protein degradation
MCM2	DNA replication licensing factor MCM2	2			1	P49736	DNA replication
EWS1/ EWSR1	Ewing sarcoma breakpoint region 1	2			1	Q01844	Uncharacterized, Transcription regulation
KIAA1967	p30/DBC protein	9				Q8N163	Apoptosis
XIRP2	Cardiomyopathy-associated protein 3	5				A4UGR9	Cytoskeleton/cell motility
CALML5	Calmodulin-like skin protein		6			Q9NZT1	Calcium signaling, Development
DEK	protein DEK isoform 1			8		P35659	Transcription regulation
THSD7A	thrombospondin type-1 domain-containing protein			5		Q9UPZ6	Uncharacterized

SMR3B	submaxillary gland androgen-regulated protein 3B	2			P02814	Extracellular processes
PDS5A	Sister chromatid cohesion protein PDS5 homolog A		2		Q29RF7	Sister chromatid cohesion, mitosis
THOC4	THO complex subunit 4	2			Q86V81	Splicing/RNA processing, Transcription regulation
CTTNBP2	cortactin-binding protein 2		2		Q8WZ74	Cytoskeleton/cell motility, Protein modification
TPR	Nucleoprotein TPR		4	3	P12270	Mitosis, protein synthesis, Nucleocytoplasmic trafficking
MCM7	DNA replication licensing factor MCM7 isoform 2		3		A4D2A2	DNA replication
MCM3	DNA replication licensing factor MCM3		2		P25205	DNA replication
MCM7	DNA replication licensing factor MCM7 isoform 1		1	1	P33993	DNA replication
MCM4	DNA replication licensing factor MCM4		1	2	P33991	DNA replication
PCNA	proliferating cell nuclear antigen		2	1	P12004	DNA replication, mitosis
TMPO	thymopoietin isoform gamma		5	4	P42167	Transcription regulation, DNA replication, mitosis
PGK1	phosphoglycerate kinase 1		2	4	P00558	Glycolysis
EVX1	Homeobox even-skipped homolog protein 1		2	2	P49640	Transcription regulation
CHD4	chromodomain-helicase-DNA-binding protein 4		1	1	Q14839	Chromatin modification/ remodeling, Transcription regulation

TABLE 2. Identification of RAD21 interactors from Immunoprecipitation-coupled Mass-spectrometry. Immunoprecipitation was performed with soluble (Sol.) and chromatin (Chr.) fractions from normal (untreated) and apoptotic (Etoposide-treated) MOLT-4 cells. *Numbers in columns indicate peptides retrieved for each protein**.**

Processes	RAD21 Interactors
Mitosis	CDC34, CLASP2, CUL4A, NCAPD2, NCAPG, PDS5A, PDS5B, PPP1R15A, PSMC1, PSMD2, RAN, RAD21, SEPT1, SMC1A, SMC2, SMC3, SMC4 , SA1, SA2, TOP3A,
Chromosome Dynamics	CHD4, HIST1H1D, NCAPD2, NCAPG, MCM2, NAP1L1, SMC2, SMC4, RFC3, SETD3
Replication	CDC34, MCM2, MCM3, MCM4, MCM7, RAD21, SMC1A, SMC2, SMC3, SMC4, TOP3A, RFC3, FEN1
RNA Processing	HNRNPH1, SYNCRIP, LPPRC, DHX9, RAN, SKIV2L2, SMC1A, THOC4, TPR, YBX1
Transcription Regulation	CDK9, CHD4, EVX1, EWS, LPPRC, MCM2, MCM3, MCM4, MCM7, NAA15, NACA3, PSPC1, RAN, YBX1, ZNF80, SETD3
Protein Modification & Degradation	CDC34, CPS1, CUL4A, DDB1, PSMC1, PSMD2, RN123, UBE2O, UBE3C
DNA Damage Response	CUL4A, DDB1, GNL1, FEN1, MCM7, PCNA, PPM1D, SMC1A, SMC3, RAD21
Apoptosis	API5, CFL1, CUL4A, CYTB, DAPK3, P30/DBC1, PPP1R15A, TNFRSF14, TBB2C
Nucleo-cytoplasmic Trafficking	KPNB1, NACA3, PCNA, RAN, TPR
Cytoskeleton & Cell Motility	ARP3 , CTTN, CTTNBP2, CLASP2, CFL1, EVL, FHL3, FLNB, TPM3, TMSB4Y, DAPK3, SEPT1, KIF3B, TUBB2C
Miscellaneous	ARG1, ACAT1, C6ORF97, CPS1, CAD, CBR1

TABLE 3. Functional classification of RAD21 interactors.

FIGURE LEGENDS

Figure 1: Validation of RAD21 interaction with candidates identified in the Y2H screen. (A) Myc-tagged RAD21 and HA-tagged FHL3 proteins were expressed in HEK293T cells as indicated, and immunoprecipitation (IP) was performed using anti-Myc agarose. RAD21 pulls down FHL3 (lane 8). **(B)** Myc-tagged RAD21 and untagged CDC34 were expressed in HEK293T cells as indicated, and IP was performed using anti-RAD21 polyclonal antibody (RAD21 pAb). The immunoprecipitates were analyzed by Western blotting using anti-RAD21 mouse monoclonal antibody (RAD21 mAb) and anti-CDC34 mouse monoclonal antibody. Inp, Input; C, Control. **(C)** Myc-tagged RAD21 is pulled down by Flag-tagged PPM1D, but not by an anti-sense construct PPM1D-AS, when expressed in HEK293T cells. **(D)** Flag-tagged RAD21 pulls down HA-tagged DAPK3 in HEK293T cells.

Figure 2: RAD21 interactors as identified by IP-Mass spectrometry. (A) A schematic for RAD21 immunoprecipitation-coupled mass spectrometry experiments. CE, cytoplasmic extract prepared by gentle hypotonic lysis of cells; NE, nuclear extract prepared by extracting isolated nuclei with NETN buffer. In a parallel experiment, total soluble proteins (soluble) were prepared by extracting MOLT-4 cells with NETN buffer; the residual pellet was sonicated to release the chromatin fraction. Asterisk (*) indicates a RAD21-negative pool. **(B)** Cellular fractionation of MOLT-4 cells. Fractionation of MOLT-4 into CE and NE and into soluble proteins (Sol.) and chromatin (Chr.) were performed in two independent experiments. α-Tubulin and Lamin B were used as markers of cytoplasmic (CE, cytoplasmic extract) and nuclear (NE, nuclear extract) fractions, respectively. Nonspecific bands are marked by asterisks (*). **(C)** Protein identifiers were analyzed with STRING, with a setting of medium confidence (0.400). Five most predictable interactors (underlined) were automatically added by selecting 'no more than 5 interactors' for additional 'interactors shown'. Black internodal lines indicate known binding, while grey lines indicate known or predicted functional interactions other than direct binding.

Figure 3: Validation of RAD21 interactors identified by IP-Mass spectrometry. (A) Endogenous RAD21 was immunoprecipitated from MOLT-4 cells and examined for the presence of proteins as indicated. **(B)** Endogenous RAD21, DDB1 and UBA1 were immunoprecipitated from MOLT-4 cells and examined as indicated. **(C)** MOLT-4 cells, untreated or treated with etoposide (10 μM, 10hr), were fractionated into total soluble proteins and chromatin fraction. Endogenous RAD21 and p30/DBC1 were immunoprecipitated and examined as indicated.

Figure 4: Affinity pull-down of proteins using Myc.RAD21 matrix. (A) Schematic for enrichment of a RAD21-cleaving activity from apoptotic MOLT-4 cells. A total of 97 proteins were identified that bound specifically to Myc.RAD21 immobilized on anti-Myc agarose, but not to anti-Myc agarose control. Nearly half of those were ribosomal proteins or translation factors. **(B)** RAD21 cleavage assay on fractions from the gel filtration (Superdex 200) column. Myc.RAD21, as substrate, was incubated with the pooled active fractions eluted from Uno S1 as input (Inp), as well as indicated fractions from the Superdex 200 column. Mock cleavage reaction (Mo) contained Myc.RAD21 substrate and the gel filtration buffer PP buffer-150. Asterisk (*) indicates the fraction (Fr. 30) that was subsequently bound to the anti-Myc agarose and anti-Myc agarose-RAD21 matrix. **(C)** Endogenous RAD21 was immunoprecipated from MOLT-4 (untreated or treated with 10μM etoposide, 10hr) whole cell lysates and examined with cohesin (RAD21, SMC1A) and condensin-I (SMC2, NCAPG) antibodies. Inp, input; C, control immunoprecipitate; IP, RAD21-immunoprecipitate. Asterisk (*) indicates apoptotic cleavage product of NCAPG.

Figure 5. Selected clusters of RAD21 interactors. (A) Chromosome architecture and dynamics, **(B)** Replication, **(C)** DNA-damage response and ubiquitination, **(D)** Transcription and RNA metabolism, **(E)** Cytoskeleton and cell motility. The clusters were generated from the composite list of interactors using DAVID, and each cluster was visualized using STRING. Interconnecting lines are based on known

interactions; thicker lines represent stronger interactions. Interaction plot was generated by STRING using a setting of medium confidence (0.400).

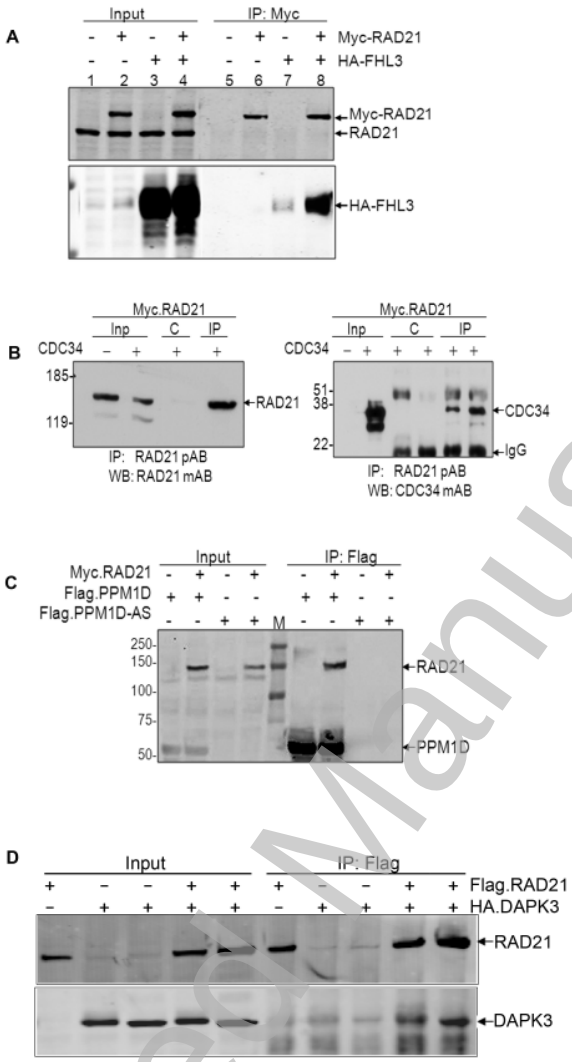

Figure 1

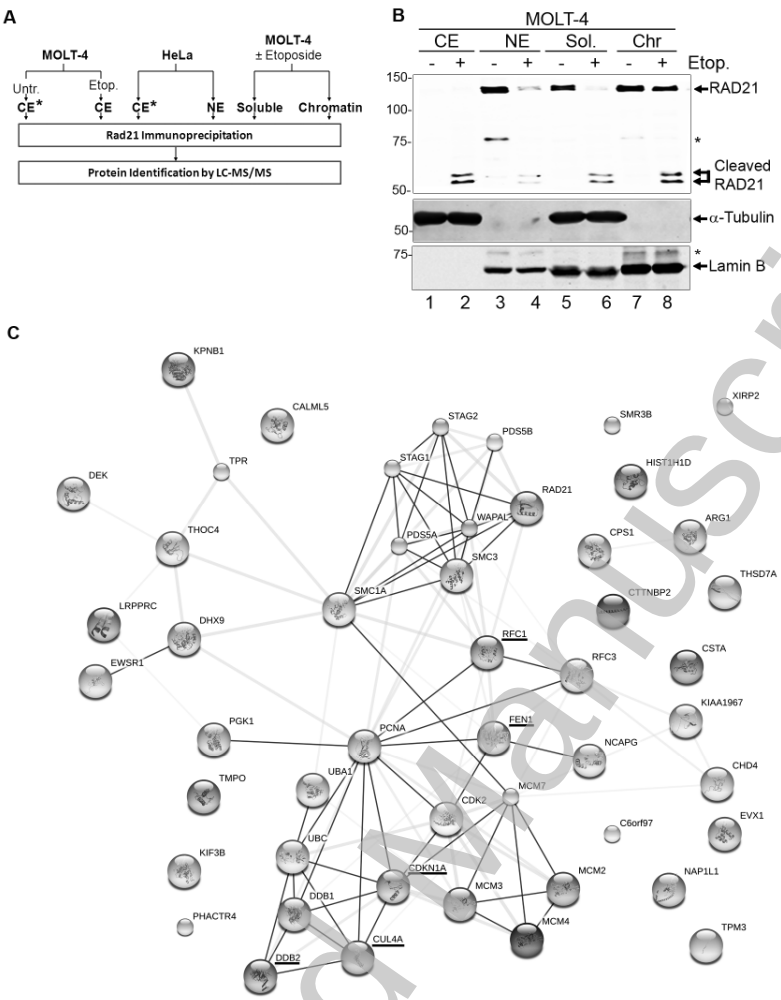

Figure 2

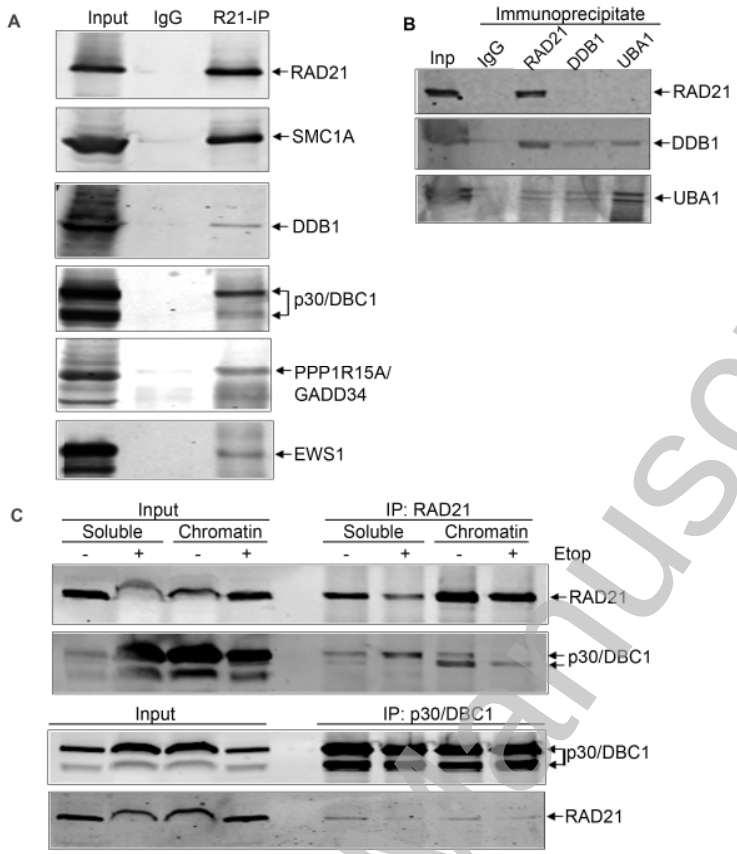

Figure 3

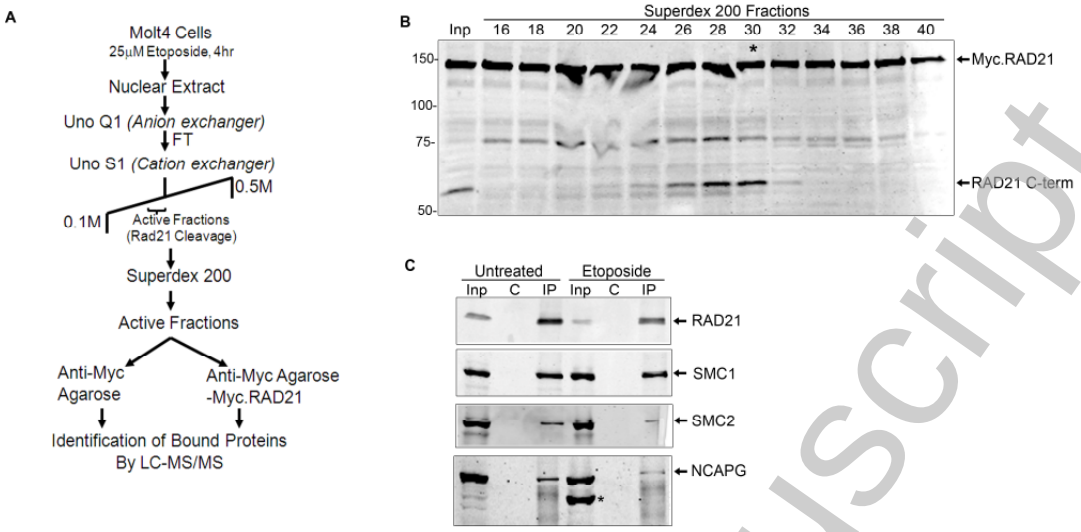

Figure 4

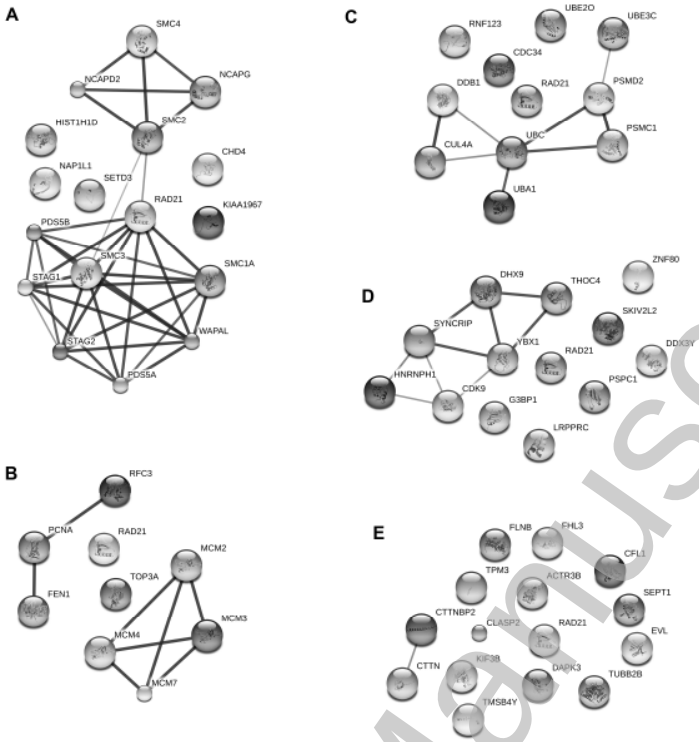

Figure 5